Electronic Structures of Nitridomanganese(V) Complexes

Christopher J. Chang, William B. Connick, Donald W. Low, Michael W. Day, and Harry B. Gray*

Arthur Amos Noyes Laboratory and the Beckman Institute, California Institute of Technology, Pasadena, California 91125

Received May 19, 1997

The single-crystal polarized absorption and circular dichroism spectra of the nitridomanganese(V) complexes (salen)Mn≡N (**1**), (1*S*,2*S*-(−)-saldpen)Mn≡N (**2**), and (1*R*,2*R*-(+)-saldpen)Mn≡N (**3**) have been measured [salen = *N*,*N*′-ethylenebis(salicylideneaminato) dianion, 1*S*,2*S*-(−)-saldpen = *N*,*N*′-(1*S*,2*S*-(−)-diphenyl)ethylenebis-(salicylideneaminato) dianion, and 1*R*,2*R*-(+)-saldpen = *N*,*N*′-(1*R*,2*R*-(+)-diphenyl)ethylenebis(salicylideneaminato) dianion]. As revealed by X-ray crystal structure analyses, these molecules have a distorted square-pyramidal geometry with a short Mn≡N bond distance (1.52(3) Å for **2**). The C_s compounds have a low-spin $^1A'[a'(x^2 - y^2)]^2$ ground state. The lowest absorption system (∼600 nm) consists of two components that are separated by approximately 4000 cm^{-1}; these are assigned to $^1A' \rightarrow {}^1A'[a'(x^2 - y^2)a'(yz)]$ (14 900 cm^{-1}) and $^1A' \rightarrow {}^1A''[a'(x^2 - y^2)a''(xz)]$ (18 900 cm^{-1}) transitions.

Introduction

Manganese coordination compounds in high oxidation states (V, VI, VII) are stabilized by strongly π-donating (oxo, imido, nitrido) ligands.[1,2] The spectroscopic properties of manganese(VII)[3−7] and manganese(VI)[8−11] complexes have been thoroughly investigated, while those of isolated d^2 manganese(V) centers remain largely unexplored.[12−15] Several stable nitridomanganese(V) porphyrins and phthalocyanines have been prepared;[16−18] however, the ligand-field transitions in the spectra of these complexes are obscured by intense intraligand bands at relatively low energies. Recently, Carreira and co-workers succeeded in characterizing the first nonmacrocyclic nitridomanganese(V) complexes by employing tetradentate Schiff bases as ancillary ligands.[19] These complexes, which are useful reagents for nitrogen transfer both to organic[19,20] and inorganic substrates,[21] exhibit ligand-field bands well to the red of ligand-based transitions, thereby allowing examination of electronic excitations involving the manganese(V) nitrido unit. Our assignments of the ligand-field transitions are based on a combination of single-crystal polarized absorption and circular dichroism (CD) spectroscopic measurements on selected compounds.[22]

Experimental Section

Preparation of Nitridomanganese(V) Compounds 1−3. The Schiff-base ligands[23−25] and their corresponding chloromanganese(III) complexes[26] were prepared according to published protocols. Complexes **1**-**3** were prepared under aerobic conditions by modification of

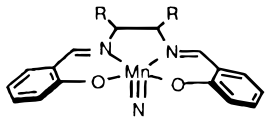

(**1**) (salen)MnN; R = H
(**2**) (1S,2S)-(-)-(saldpen)MnN; R = Ph
(**3**) (1R,2R)-(+)-(saldpen)MnN; R = Ph

the method of Carreira et al.[19] The chloromanganese(III) derivative (0.50 mmol, 1 equiv) was dissolved in dichloromethane/methanol (4:1, 50 mL). Ammonium hydroxide (15 M, 15 mmol, 15 equiv) was added in one portion, and the mixture was stirred vigorously for 15

(1) Nugent, W. A.; Mayer, J. M. *Metal−Ligand Multiple Bonds*; Wiley-Interscience: New York, 1988.
(2) Lever, A. B. P. *Inorganic Electronic Spectroscopy*; Elsevier Science Publishers B.V.: Amsterdam, 1984.
(3) Viste, A.; Gray, H. B. *Inorg. Chem.* **1964**, *3*, 1113−1123.
(4) Schatz, P. N.; McCaffery, A. J.; Suetaka, W.; Henning, G. N.; Ritchie, B.; Stephens, P. J. *J. Chem. Phys.* **1966**, *45*, 722−734.
(5) Holt, S. L.; Ballhausen, C. J. *Theor. Chim. Acta* **1967**, *7*, 313−320.
(6) Day, P.; DiSipio, L.; Oleari, L. *Chem. Phys. Lett.* **1970**, *5*, 533−536.
(7) Homberg, H. Z. *Anorg. Chem.* **1983**, *498*, 25−40.
(8) DiSipio, L.; Oleari, L.; Day, P. *J. Chem. Soc., Faraday Trans. 2* **1972**, *68*, 776−792.
(9) Milstein, J. B.; Ackerman, J.; Holt, S. L.; McGarvey, B. R. *Inorg. Chem.* **1972**, *11*, 1178−1184.
(10) Kosky, C. A.; McGarvey, B. R.; Holt, S. L. *J. Chem. Phys.* **1972**, *56*, 5904−5912.
(11) Day, P.; DiSipio, L.; Ingletto, G.; Oleari, L. *J. Chem. Soc., Dalton Trans.* **1973**, 2595−2605.
(12) Borromei, R.; Oleari, L.; Day, P. *J. Chem. Soc., Faraday Trans. 2* **1977**, *73*, 135−146.
(13) Borromei, R.; Oleari, L.; Day, P. *J. Chem. Soc., Faraday Trans. 2* **1981**, *77*, 1563−1578.
(14) Collins, T. J.; Powell, R. D.; Slebodnick, C.; Uffelman, E. S. *J. Am. Chem. Soc.* **1990**, *112*, 899−901.
(15) Niemann, A.; Bossek, U.; Haselhorst, G.; Wieghardt, K.; Nuber, B. *Inorg. Chem.* **1996**, *35*, 906−915.
(16) Hill, C. L.; Hollander, F. J. *J. Am. Chem. Soc.* **1982**, *104*, 7318−7319.
(17) Buchler, J. W.; Dreher, C.; Lay, K.-L.; Lee, Y. J. A.; Scheidt, W. R. *Inorg. Chem.* **1983**, *22*, 888−891.
(18) Groves, J. T.; Takahashi, T. *J. Am. Chem. Soc.* **1983**, *105*, 2073−2074.
(19) Du Bois, J.; Hong, J.; Carreira, E. M.; Day, M. W. *J. Am. Chem. Soc.* **1996**, *118*, 915−916.
(20) Du Bois, J.; Tomooka, C. S.; Hong, J.; Carreira, E. M. *J. Am. Chem. Soc.* **1997**, *119*, 3179−3180.
(21) Chang, C. J.; Low, D. W.; Gray, H. B. *Inorg. Chem.* **1997**, *36*, 270−271.
(22) Salen = *N*,*N*′-ethylenebis(salicylideneaminato) dianion; 1*S*,2*S*-(−)-saldpen = *N*,*N*′-(1*S*,2*S*-(−)-diphenyl)ethylenebis(salicylideneaminato) dianion; 1*R*,2*R*-(+)-saldpen = *N*,*N*′-(1*R*,2*R*-(+)-diphenyl)ethylenebis-(salicylideneaminato) dianion.
(23) Mason, A. T. *Chem. Ber.* **1887**, *20*, 271−277.
(24) Pfeiffer, P.; Breith, E.; Lübbe, E.; Tsumaki, T. *Liebigs Ann. Chem.* **1933**, *503*, 84−129.
(25) Pfeiffer, P.; Thielert, H. *J. Prakt. Chem.* **1937**, *149*, 242−296.
(26) Zhang, W.; Jacobsen, E. N. *J. Org. Chem.* **1991**, *56*, 2296−2298.

S0020-1669(97)00598-3 CCC: $15.00
Published on Web 05/28/1998

min. Clorox bleach (6 equiv) was added dropwise to the mixture, and the resulting biphasic suspension was stirred at room temperature until the reaction mixture turned green. The product was extracted with dichloromethane, washed with water (5 × 25 mL), and concentrated to yield the crude nitrido complex. Purification by flash column chromatography (neutral aluminum oxide, dichloromethane/hexane) gave analytically pure product as emerald-green microcrystals (70−80% yield). Elemental analyses (C, H, N) were performed by Galbraith Laboratories (Knoxville, TN). Characterization data for **1**: ^{1}H NMR (CD_2Cl_2, 500 MHz) δ 8.01 (s, 2H, N=C−H), 7.32 (dt, 2H, J = 7.3, 1.3 Hz, Ar−H), 7.19 (dd, 2H, J = 6.8, 1.7 Hz, Ar−H), 6.89 (d, 2H, J = 8.4 Hz, Ar−H), 6.65 (t, 2H, J = 7.2 Hz, Ar−H), 3.81 (m, 2H, CH_2), 3.66 (m, 2H, CH_2). Calcd (found) for $C_{16}H_{14}N_3O_2Mn$: C, 56.44 (56.30); H, 4.20 (4.20); N, 12.53 (12.37).

Characterization data for **2**: ^{1}H NMR δ 7.66 (d, 2H, J = 27.1 Hz, N=C−H), 7.29 (m, 10H, Ar−H), 7.17 (m, 4H, Ar−H), 6.94 (m, 4H, Ar−H), 6.56 (m, 2H, Ar−H), 5.00 (dd, 4H, J = 55.5, 10 Hz, CH_2). Calcd (found) for $C_{28}H_{22}N_3O_2Mn$: C, 68.99 (68.18); H, 4.51 (4.82); N, 8.62 (8.18).

Characterization data for **3**: ^{1}H NMR δ 7.66 (d, 2H, J = 27.1 Hz, N=C−H), 7.29 (m, 10H, Ar−H), 7.17 (m, 4H, Ar−H), 6.94 (m, 4H, Ar−H), 6.56 (m, 2H, Ar−H), 5.00 (dd, 4H, J = 55.5, 10 Hz, CH_2). Calcd (found) for $C_{28}H_{22}N_3O_2Mn$: C, 68.99 (68.83); H, 4.51 (4.77); N, 8.62 (8.68).

Physical Measurements. ^{1}H NMR spectra were recorded using a Bruker AM-500 spectrometer. Solution absorption spectra were obtained using either a Cary 14 spectrophotometer upgraded by On-Line Instrument Systems (OLIS) to include computer control or a Hewlett-Packard 8452A diode array spectrophotometer. Circular dichroism spectra were recorded with a JASCO J-600 CD spectropolarimeter. Polarized absorption spectra were measured using a home-built diode array spectrophotometer (xenon or tungsten filament sources) modified for handling small crystalline samples.[27] Crystals of **1** were grown from a slow evaporating dichloromethane solution. Unit-cell dimensions for **1** were obtained from the setting angles of 12 reflections using an Enraf-Nonius CAD-4 diffractometer (graphite monochromator and Mo Kα radiation). Observed (previously reported)[19] for **1**: monoclinic, space group $P2_1/c$, a = 9.496(3), b = 12.313(3), c = 12.857(4) Å; β = 103.61° (3). Single crystals for absorption measurements were mounted on nickel disks containing apertures smaller than the size of the crystals. Polarized spectra were recorded with light incident on the [100] plane, parallel and perpendicular to the crystallographic b axis ($||b$ and $\perp b$, respectively). All spectroscopic measurements were made at room temperature.

X-ray Crystallography of (1*S*,2*S*-(−)-saldpen)Mn≡N•3CH$_3$CN (2). Green crystals were grown by slow evaporation of an acetonitrile solution. A single crystal (0.4 × 0.4 × 0.2 mm) was mounted on a glass fiber. Diffraction data were collected at 160 K using an Enraf-Nonius CAD-4 diffractometer (graphite monochromator and Mo Kα radiation, λ = 0.710 73 Å). Intensity data were collected in the range of 2° < θ < 25°. Diffraction data were corrected for Lorentz and polarization effects. The intensities of three standard reflections showed no variations greater than those predicted by counting methods. Lattice parameters were determined from the setting angles of 25 independent reflections. Ligand hydrogen atoms were included at calculated positions (C−H, 0.95 Å) with fixed isotropic displacement parameters. All other atoms were refined anisotropically. The structure was solved using direct methods in SHELXS-86[28] and refined using SHELXL-93.[29] Plots were drawn using ORTEP.[30] Pertinent data are included in Table 1 and Supporting Information.

Table 1. Crystallographic Data for (1*S*,2*S*-(−)-saldpen)Mn≡N·3CH$_3$CN (**2**)

formula = $C_{28}H_{22}MnN_3O_2$·1.5(C_2H_3N)	fw = 549.01
a = 20.924(4) Å	space group: $C2$ (No. 5)
b = 18.197(5) Å	ρ_{calc} = 1.35 g/cm^3
c = 17.238(3) Å	μ = 5.25 cm^{-1} (θ_{max} = 25°)
β = 124.60(2) Å	9295 ind relfcns (+h, ±k, ±l)
V = 5403(2) Å^3	T = 160 K
Z = 8	$R1^a$, w$R2^b[I > 2\sigma(I)]$ = 0.0504, 0.0895
GOF^c = 1.49 (649 params)	$R1^a$, w$R2^b$(all data) = 0.0649, 0.0932

^{a} $R1 = \sum||F_o| - |F_c||/\sum|F_o|$. ^{b} w$R2 = (\sum(w(F_o^2 - F_c^2)^2)/\sum(w(F_o^2)^2))^{1/2}$. ^{c} GOF = $(\sum w(F_o^2 - F_c^2)^2/(n-p))^{1/2}$ where n is the number of data and p is the number of parameters refined.

Chart 1

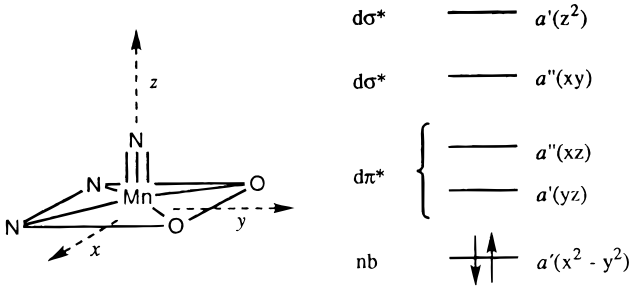

Results and Discussion

The electronic structures of nitridomanganese(V) complexes are readily described in terms of the ligand-field model that was developed to account for the absorption spectrum of the hydrated vanadyl ion, $VO(H_2O)_5^{2+}$.[31] A similar treatment has been applied to Re(V) and Tc(V) *trans*-dioxo compounds;[32−34] such complexes may be regarded as spectroscopic analogues of the C_s d^2 nitridomanganese(V) derivatives. The electronic structures of these nitridomanganese(V) Schiff-base complexes are of particular interest because it is likely that the lowest ligand-field excited states of C_{4v} d^2 osmium(VI) nitrido analogues undergo a molecular distortion to a C_{2v} structure.[35,36] For the low-symmetry C_s system studied here, inequivalent π interactions between the Mn≡N chromophore and the salen ligands remove the degeneracy of the d_{xz} and d_{yz} orbitals. A ligand-field splitting diagram for an axially compressed C_s complex is shown in Chart 1.

In the $^1A'[a'(x^2 - y^2)]^2$ ground state, the formally nonbonding $a'(x^2 - y^2)$ level is filled. The unoccupied dπ* levels, $a'(yz)$ and $a''(xz)$, have Mn≡N π-antibonding character. The higher-lying $a''(xy)$ and $a'(z^2)$ orbitals are σ-antibonding. The lowest excited states should be $^{3,1}A'[a'(x^2 - y^2)a'(yz)]$ and $^{3,1}A''[a'(x^2 - y^2)a''(xz)]$; since the spin−orbit coupling in ^{3}MnN is expected to be relatively small,[37] transitions to the triplet states will be very weak.

The emerald green (salen)Mn≡N complex (**1**) is remarkably stable to both air and water and is slightly soluble in common

(27) Libowitzky, E.; Rossman, G. R. *Phys. Chem. Miner.* **1996**, *23*, 319−327.
(28) Sheldrick, G. M. *SHELXS-86*; Universität Göttingen: Göttingen, Germany, 1990.
(29) Sheldrick, G. M. *SHELXL-93*; Universität Göttingen: Göttingen, Germany, 1993.
(30) Johnson, C. K. *ORTEPII*; Report ORNL-5138; Oak Ridge National Laboratory: Oak Ridge, TN, 1976.
(31) Ballhausen, C. J.; Gray, H. B. *Inorg. Chem.* **1962**, *1*, 111−122.
(32) Winkler, J. R.; Gray, H. B. *J. Am. Chem. Soc.* **1983**, *105*, 1373−1374.
(33) Winkler, J. R.; Gray, H. B. *Inorg. Chem.* **1985**, *24*, 346−355.
(34) Miskowski, V. M.; Gray, H. B.; Hopkins, M. D. *Adv. Trans. Met. Coord. Chem.* **1996**, *1*, 159−186.
(35) Hopkins, M. D.; Miskowski, V. M.; Gray, H. B. *J. Am. Chem. Soc.* **1986**, *108*, 6908−6911.
(36) Cowman, C. D.; Trogler, W. C.; Mann, K. R.; Poon, C. K.; Gray, H. B. *Inorg. Chem.* **1976**, *15*, 1747−1751.
(37) The spin−orbit coupling constant extracted from analysis of the EPR spectrum of a closely related d^1 complex, (salen)Cr≡N, is only 106 cm^{-1}: Azuma, N.; Imori, Y.; Yoshida, H.; Tajima, K.; Li, Y.; Yamauchi, J. *Inorg. Chim. Acta* **1997**, *266*, 29.

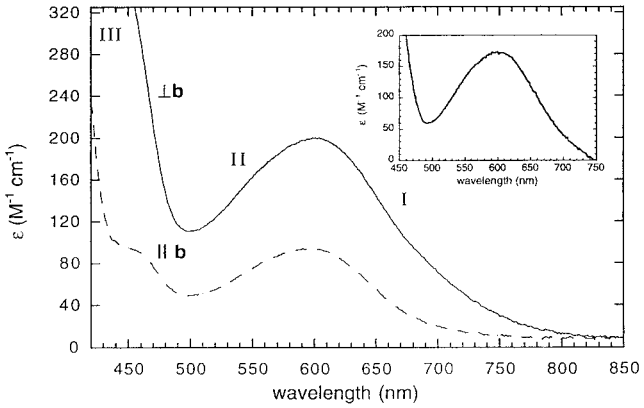

Figure 1. Single-crystal polarized absorption spectra of (salen)Mn≡N (**1**). With light incident on the [100] face, the ||*b*- and ⊥*b*-labeled spectra correspond to polarizations parallel and perpendicular to the *b* axis, respectively. The molecular *z* axis (defined by the Mn≡N bond vector) is roughly aligned along the *b* axis (inclination angle, 26.7°). Inset shows an expanded view of the lowest-energy band system in dichloromethane solution.

organic solvents (dichloromethane, acetonitrile, dimethylformamide). The previously reported crystal structure of **1** establishes that the monomeric complex adopts a distorted square-pyramidal geometry with a Mn≡N bond length of 1.512(3) Å; the Mn is raised 0.492(2) Å out of the plane defined by the coordinating N and O atoms of the salen ligand. The visible region of the solution absorption spectrum of **1** (inset Figure 1) is dominated by a weak, broad, and asymmetric system near 600 nm (ϵ 150 M^{-1} cm^{-1}). Owing to its position and intensity, this system is assigned to spin-allowed $a'(x^2 - y^2) \rightarrow d\pi^*$ transitions, $^1A' \rightarrow {}^1A',{}^1A''$, and its band shape can be interpreted in terms of the $^1A'[a'(yz)]$ and $^1A''[a''(xz)]$ split components. Not surprisingly, this system occurs to the red of the maxima of the corresponding transitions in the solution spectra of Tc(V) and Re(V) *trans*-dioxo compounds (~450 nm).[32−34] The higher-lying ligand-field transitions of **1** are obscured by intense charge-transfer bands in the UV region. Notably, an asymmetric feature near 380 nm (ϵ = 6100 M^{-1} cm^{-1}) is attributable to intraligand azomethine transitions, and the intense features near 300 (ϵ = 15 000 M^{-1} cm^{-1}) and 230 nm (ϵ = 30 000 M^{-1} cm^{-1}) are due to ligand $\pi \rightarrow \pi^*$ transitions.[38−40]

The single-crystal polarized absorption spectra of **1** are shown in Figure 1. The monoclinic crystals[19] are strongly dichroic; thin plates viewed perpendicular to the [100] face are nearly colorless with transmitted light polarized parallel to the *b* axis (||*b*) and deep green with light polarized perpendicular to the *b* axis (⊥*b*). The broad 600 nm feature that is observed in the solution absorption spectrum is strongly polarized ⊥*b*. Since the molecular *z* axis, defined by the Mn≡N bond vector, is roughly aligned along the *b* axis (inclination angle, 26.7°), the electronic transitions comprising the 600 nm envelope are strongly polarized in the molecular *x*,*y* plane. Inspection of the ||*b* and ⊥*b* spectra reveals that the low-energy flank of the absorption system is more strongly polarized than the high-energy flank. These data are consistent with two overlapping bands with maxima near 670 (band I) and 540 nm (band II). The estimated energy spacing between the band maxima (~3600 cm^{-1}) is attributable to the splitting of the $^1A'[a'(x^2 - y^2)a'(yz)]$ and $^1A''[a'(x^2 - y^2)a''(xz)]$ excited states, implying $d\pi^*$ splittings similar to those for analogous low-spin d^7 Co(II) Schiff-base complexes.[41,42] In contrast, splittings of the singlet states derived from $a'(x^2 - y^2) \rightarrow d\pi^*$ transitions are not resolved in the single-crystal spectra of D_{4h} Tc(V) and Re(V) *trans*-dioxo complexes.[32−34] From group theoretical considerations, transitions to the $^1A'[a'(x^2 - y^2)a'(yz)]$ and $^1A''[a'(x^2 - y^2)a''(xz)]$ excited states are expected to be *y*,*z*- and *x*-polarized, respectively. In fact, the measured extinction coefficients, $\epsilon_{||}$ and $\epsilon_{\perp}$, and polarization ratios for **1** are consistent with the assignment of band I to the $^1A' \rightarrow {}^1A'[a'(x^2 - y^2)a'(yz)]$ transition with *y* and partial *z* polarization. Similarly, band II may be attributed to the *x*-polarized $^1A' \rightarrow {}^1A''[a'(x^2 - y^2)a''(xz)]$ transition. The derived orbital energy sequence $a'(yz) < a''(xz)$ is in agreement with that observed for Co(salen).[41,42] Interestingly, the single-crystal absorption data also reveal a strongly *xy*-polarized shoulder near 450 nm (band III) that is not resolved in the solution spectrum; we tentatively assign this band to the $^1A' \rightarrow {}^1A''[a'(x^2 - y^2)a''(xy)]$ transition.[43]

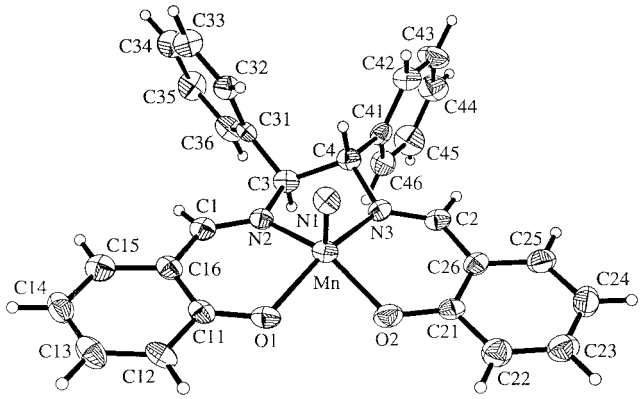

Figure 2. ORTEP[30] diagram of one of the two independent molecules in the unit cell of (1*S*,2*S*-(−)-saldpen)Mn≡N·3CH_3CN (**2**). Thermal ellipsoids are drawn at the 50% probability level showing the atom numbering scheme. Hydrogen atoms are depicted as spheres of arbitrary size.

Further insight into the electronic structures of the nitridomanganese(V) complexes is provided by the spectroscopy of the chiral analogues (1*S*,2*S*-(−)-saldpen)Mn≡N (**2**) and (1*R*,2*R*-(+)-saldpen)Mn≡N (**3**). In these complexes, two chiral centers are incorporated into the ethylene backbone of the salen ligand by replacing a hydrogen on each carbon with a phenyl group. The structure of **2** was confirmed by single-crystal X-ray analysis (Figure 2). The complex is five-coordinate with a distorted square-pyramidal geometry similar to that of **1**. There are two molecules in the asymmetric unit. The Mn≡N bond

(38) Bosnich, B. *J. Am. Chem. Soc.* **1968**, *90*, 627−632.
(39) Braithwaite, A. C.; Waters, T. N. *J. Inorg. Nucl. Chem.* **1973**, *35*, 3223−3229.
(40) Braithwaite, A. C.; Wright, P. E.; Waters, T. N. *J. Inorg. Nucl. Chem.* **1975**, *37*, 1669−1674.
(41) Ceulemans, A.; Dendooven, M.; Vanquickenborne, L. G. *Inorg. Chem.* **1985**, *24*, 1159−1165.
(42) Hitchman, M. A. *Inorg. Chem.* **1977**, *16*, 1985−1993.
(43) The morphology of the crystal and handling difficulties precluded direct determination of the two optical axes perpendicular to *b*. However, the orientation of these axes is readily expressed in terms of a single parameter ϕ (rotation angle about *b*), allowing the formulation of the polarization ratio *R* ($abs_{\perp}/abs_{||}$) in terms of ϕ for an electric dipole-allowed transition polarized along a single molecular axis. Estimating the isotropic extinction as three times the solution value, values of $\epsilon_{\perp}$ and $\epsilon_{||}$ can be predicted as a function of ϕ. From this analysis it is apparent that the 670 nm band (R_{obs} = 3.3) is not uniquely *x*-polarized and must be at least partially *y*-polarized. In contrast, the R_{obs} for the 540 nm band (2.4) is consistent with an *x*-polarized transition. Choosing ϕ such that R_{calc} is 2.4 for an *x*-polarized band at 540 nm, the calculated $\epsilon_{\perp}$ and $\epsilon_{||}$ values are 159 and 66 M^{-1} cm^{-1}, respectively (observed: 146 and 56 M^{-1} cm^{-1}). If the 670 nm band is *y*-polarized and partially *z*-polarized (13%), the calculated $\epsilon_{\perp}$ and $\epsilon_{||}$ values are 89 and 25 M^{-1} cm^{-1}, respectively (observed: 106 and 31 M^{-1} cm^{-1}).

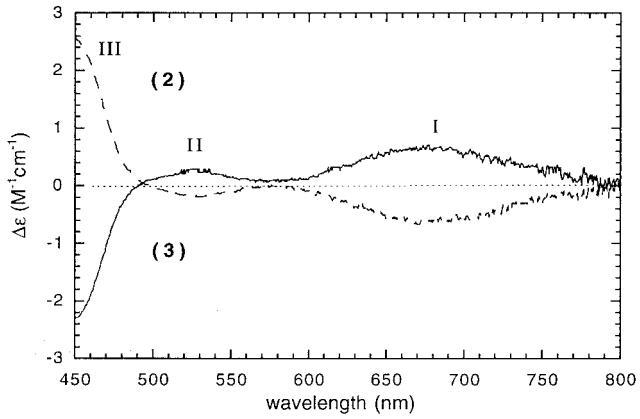

Figure 3. Circular dichroism spectra of (1*S*,2*S*-(−)-saldpen)Mn≡N (**2**) and (1*R*,2*R*)-(+)-saldpen)Mn≡N (**3**) in dichloromethane solution.

length is 1.52 Å (1.509(3) and 1.531(3) Å), and the Mn is raised 0.47 Å (0.466(1) and 0.480(2) Å) out of the plane defined by the coordinating atoms of the chelate. As expected, these ligand modifications have little impact on the energies of the $a'(x^2 - y^2) \rightarrow d\pi^*$ excited states, and the solution visible absorption spectra of **2** and **3** are similar to the spectrum of **1**.[44] However, the chiral groups produce the dissymmetry necessary to make the metal-centered $a'(x^2 - y^2) \rightarrow d\pi^*$ transitions optically active, and the resulting CD spectra are striking (Figure 3). The 600 nm feature is cleanly resolved into two CD bands (bands I and II, 670 and 530 nm, respectively). The energy spacing between band maxima (~3900 cm^{-1}) is in good agreement with the splitting of the $a'(x^2 - y^2) \rightarrow d\pi^*$ transitions deduced from the single-crystal spectra of **1**.[45,46] The signal for the lower energy CD feature ($\Delta\epsilon = 0.7\ M^{-1}\ cm^{-1}$) is considerably stronger than that of the higher energy band ($\Delta\epsilon = 0.3\ M^{-1}\ cm^{-1}$). From spatial considerations the $^1A' \rightarrow {}^1A'[a'(x^2 - y^2)a'(yz)]$ transition is expected to be more strongly influenced by the vicinal chiral groups than is the $^1A' \rightarrow {}^1A''[a'(x^2 - y^2)a''(xz)]$ transition; thus, the relative intensities confirm the energy ordering $^1A' \rightarrow {}^1A' < {}^1A' \rightarrow {}^1A''$ for these excitations. Band III appears as a solvent-insensitive shoulder near 450 nm. The UV region features intense intraligand excitations corresponding to those seen in the solution absorption spectra.[47−50]

Acknowledgment. We thank J. Du Bois, L. Henling, J. Hong, G. Rossman, and T. Takeuchi for expert technical assistance as well as several helpful discussions. C.J.C. thanks the A. A. Noyes Foundation for a Caltech SURF award. D.W.L. acknowledges the Parsons Foundation for a fellowship. This work was supported by the National Science Foundation.

Supporting Information Available: Tables giving complete crystallographic experimental details, distances and angles, positional parameters for all atoms, additional ORTEP[30] unit cell diagrams, and anisotropic displacement parameters for **2** (12 pages). See any current masthead page for ordering instructions.

IC970598K

(44) Complexes **2** and **3** give identical solution absorption spectra. The visible region of the solution absorption spectra of **2** and **3** feature a similar ligand-field band system as observed for **1** (602 nm, $\epsilon = 170\ M^{-1}\ cm^{-1}$). The asymmetric near-UV absorption, corresponding to intraligand azomethine transitions, is slightly red-shifted (380 nm for **1**, 386 nm for **2** and **3**). The higher-lying intraligand transitions are observed at similar energies for all three complexes.

(45) The relationship between absorption and CD band shapes and maxima has been discussed previously: Moffitt, W.; Moscowitz *J. Chem. Phys.* **1959**, *30*, 648−660.

(46) Kauzmann, W. J.; Walter, J. E.; Eyring, H. *Chem. Rev.* **1940**, *26*, 339−407.

(47) Molecular orbital calculations and previous experimental studies suggest that the lowest energy $\pi-\pi^*$ transition involves orbitals that originate from the ligand azomethine group (refs 38−40). It is interesting to note that the split signal found in the CD spectrum, as well as the asymmetry in the corresponding absorption band, may be attributed to exciton (Davydov) interactions that give rise to nondegenerate $\pi-\pi^*$ transitions of the azomethine chromophore.

(48) Moffitt, W. *J. Chem. Phys.* **1956**, *25*, 467−478.

(49) Levinson, G. S.; Simpson, W. T.; Curtis, W. *J. Am. Chem. Soc.* **1957**, *79*, 4314−4320.

(50) Mason, S. F.; Vane, G. W. *Tett. Lett.* **1965**, *21*, 1593−1597.